J|A|C|S
ARTICLES
Published on Web 04/25/2002

A Structural Model for the High-Valent Intermediate Q of Methane Monooxygenase from Broken-Symmetry Density Functional and Electrostatics Calculations

Timothy Lovell,* Wen-Ge Han,* Tiqing Liu, and Louis Noodleman*

Contribution from the Department of Molecular Biology, The Scripps Research Institute, La Jolla California 92037

Received September 6, 2001. Revised Manuscript Received January 29, 2002

Abstract: A combined broken-symmetry density functional and electrostatics approach has been used to construct a model for the high-valent diiron intermediate Q of methane monooxygenase. The presence of high-spin or intermediate spin iron centers gives rise to two structurally distinct spin-coupled states of the cluster for which calculated geometries, net spin populations, Heisenberg *J* values, Mössbauer isomer shifts, and quadrupole splittings are compared and contrasted with the available spectroscopic data.

Introduction

Soluble methane monooxygenase (MMO) is a protein that belongs to a class of binuclear non-heme iron enzymes capable of activating dioxygen for further oxidation chemistry.[1] The hydroxylase component (MMOH) of the MMO protein selects specifically for the reaction in which methane is converted to methanol and water via reaction with O_2 and NADH. The catalytic cycle of MMOH is well-established.[2,3] Coupled electron and proton addition to the Fe(III)Fe(III) resting enzyme generates the reduced Fe(II)Fe(II) state. Two spectroscopically observable intermediates, P and Q, are then formed upon reaction with dioxygen. Q is the proposed high-valent Fe(IV)-Fe(IV) species capable of oxidizing methane. Presently, no X-ray structure of the protein exists that contains intermediate Q and no Fe(IV)Fe(IV) model complexes with biologically relevant ligands have been stabilized in aqueous solution.[1] The identity of intermediate Q is thus an unknown quantity but a topic of substantial interest.

Freeze-quench trapping techniques coupled with Mössbauer and EXAFS spectroscopies have provided the most insight into possible structures for Q.[4−8] Mössbauer data indicate that Q exhibits diamagnetism at high magnetic field strength[6] and comprises two near-equivalent Fe(IV) sites that are antiferromagnetically coupled ($J < -30$ cm^{-1}).[5,6] XAS experiments on *M. trichosporium* indicate preedge areas consistent with Fe coordination numbers of 5 or lower.[7] EXAFS spectra from *M. trichosporium* suggest a diamond core (Fe_2O_2) exists comprising one short (1.77 Å) and one long (2.06 Å) bond to each Fe and an Fe−Fe distance ranging from 2.46 to 2.52 Å.[7,8] In attempting to construct a quantum chemical model that accurately represents intermediate Q, our working hypothesis is that the active site cluster be consistent with most of the experimental observations noted above.

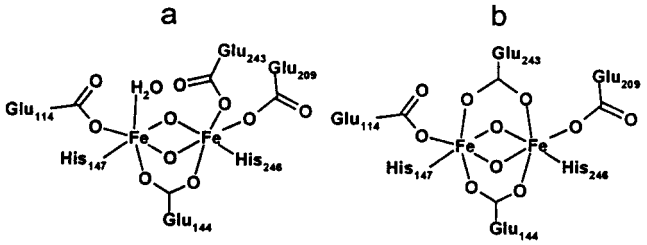

Figure 1. Core structures of DFT-proposed active sites for intermediate Q from (a) Gherman et al.[9] and (b) Siegbahn.[10,11]

Theoretical proposals to model intermediate Q have led to a number of plausible structures. The majority have been discounted on geometric and energetic grounds and because most fail to meet the spectroscopic criteria. Promising core structures have been put forward by Gherman et al.[9] and Siegbahn[10,11] (Figure 1a,b), from which the energetics associated with methane binding and activation have been explored. As a first step to modeling intermediate Q, we have also performed calculations on these models. The question we have asked is to what extent does the protein and solvent environment modify their proper-

* To whom correspondence should be addressed. E-mail: tlovell@scripps.edu, wengehan@scripps.edu, and lou@scripps.edu. Fax: +1 858 784 8896.

(1) Solomon, E. I.; Brunold, T. C.; Davis, M. I.; Kemsley, J. N.; Lee, S.-K.; Lehnert, N.; Neese, F.; Skulan, A. J.; Yang, Y.-S.; Zhou, J. *Chem. Rev.* **2000**, *100*, 235−349 and references therein.
(2) Liu, K. E.; Lippard, S. J. *Adv. Inorg. Chem.* **1995**, *42*, 263−289.
(3) Wallar, B. J.; Lipscomb, J. D. *Chem. Rev.* **1996**, *96*, 2625−2657.
(4) Liu, K. E.; Valentine, A. M.; Wang, D.; Huynh, B. H.; Edmondson, D. E.; Salifoglou, A.; Lippard, S. J. *J. Am. Chem. Soc.* **1995**, *117*, 10174−101.
(5) Liu, K. E.; Wang, D.; Huynh, B. H.; Edmondson, D. E.; Salifoglou, A.; Lippard, S. J. *J. Am. Chem. Soc.* **1994**, *116*, 7465−7466.
(6) Lee, S.-K.; Fox, B. G.; Froland, W. A.; Lipscomb, J. D.; Münck, E. *J. Am. Chem. Soc.* **1993**, *115*, 6450−6451.
(7) Shu, L.; Nesheim, J. C.; Kauffmann, K.; Münck, E.; Lipscomb, J. D.; Que, L., Jr. *Science* **1997**, *275*, 515−517.
(8) Hsu, H.-F.; Dong, Y.; Shu, L.; Young, V. G., Jr.; Que, L., Jr. *J. Am. Chem. Soc.* **1999**, *121*, 5230−5237.
(9) Gherman, B. F.; Dunietz, B. D.; Whittington, D. A.; Lippard, S. J.; Friesner, R. A. *J. Am. Chem. Soc.* **2001**, *123*, 3836−3837.
(10) Siegbahn, P. E. M. *Inorg. Chem.* **1999**, *38*, 2880−2889.
(11) Siegbahn, P. E. M. *JBIC, J. Biol. Inorg. Chem.* **2001**, *6*, 27−45.

10.1021/ja0121282 CCC: $22.00

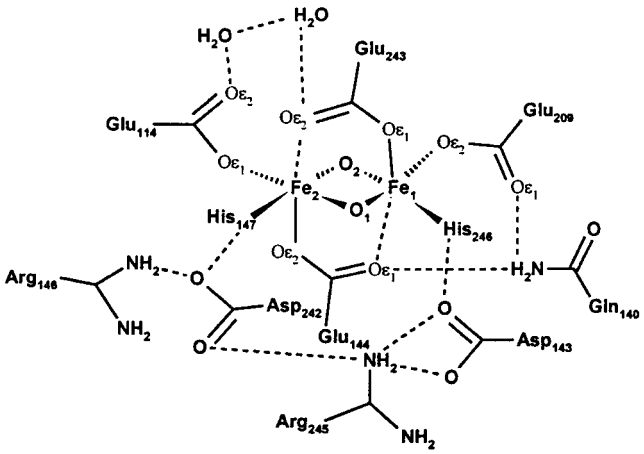

Figure 2. Proposed active site model for intermediate Q from combined broken-symmetry DFT and electrostatics calculations.

ties? The combined effect of a number of protein residues in an extended quantum model developed from those in Figure 1 is examined herein.

Our quantum model of Q was originally guided by broken symmetry density functional and electrostatics calculations on the electroneutral clusters (shown in Figure 1) placed in chain D of the *M. capsulatus* protein.[12,13] A number of second- and third-shell amino acid residues (Asp143, Asp242, Gln140, Arg245, and Arg146) appear to be structurally, electrostatically, and therefore energetically significant. A second shell water molecule (Wat785 from oxidized *M. capsulatus*) thought to play a key role in the conversion of the Fe(III)Fe(III) form to the Fe(II)Fe(II) state is also included.[12,13] Our model of Q containing 102 atoms is shown in Figure 2.

The primary goal of developing this complementary model is to rationalize to what extent the properties of the active site are governed by the spin state ($S = 2$, high spin (HS) *or* $S = 1$, intermediate spin (IS)) of the individual Fe sites when second- and third-shell amino acid ligands are present and so to incorporate the majority of the long-range protein and solvent environment effects within the quantum mechanics. The characteristic features of Q of most interest that we examine include the geometry (Fe−Fe distance) and Fe coordination number, Fe net spin populations, relative energies between spin states, the exchange coupling between the two Fe sites, and the spectroscopically observed Mössbauer isomer shifts and quadrupole splittings.

Computational Details

The Amsterdam Density functional package (ADF, version 2.3)[14] was used to compute the geometries and energies of the active site clusters. For all calculations, ADF basis set IV was used to model all atoms. This corresponds to uncontracted triple-ζ Slater-type orbitals (STO) for the 3s, 3p, 3d, and 4s valence orbitals of Fe with a 4p polarization orbital, triple-ζ STOs for 2s, 2p valence orbitals of C, N, O augmented with a 3d polarization orbital, and triple-ζ STO for 1s of H with a 2p polarization orbital.[15] The inner core orbitals were treated by the frozen core approximation. An auxiliary charge density fit set that consists of s, p, d, f, and g STO functions was adopted to fit the molecular density and used to calculate the Coulomb and exchange potentials.[16] The numerical integration scheme was the polyhedron method developed by te Velde et al.[17] The analytical gradient method implemented by Versluis et al.[18] was used along with a numerical integration accuracy of 4.0. Optimizations used the Newton−Raphson method and the Hessian was updated with the Broyden Fletcher Goldfard Shanno scheme.[19] Convergence criteria were set to 0.001 Å in coordinates and 0.01 hartree/Å in the norm of all gradient vectors. All calculations were done using the spin-unrestricted method at the GGA level (Vosko−Wilk−Nusair (VWN) parametrization for the LDA)[20] with the generalized gradient correction terms included in the SCF as introduced by Perdew and Wang (PW91)[21] to the exchange and correlation. The broken symmetry (BS) approach[22] was used to model the antiferromagnetic (AF) coupling between the Fe sites. To construct a BS state, a high-spin (HS) or intermediate-spin (IS) state calculation was first completed. The SCF converged fit density of the HS or IS states was then manipulated by exchanging blocks of α and β electron densities. In this way, the starting potential for the required spin-flipped AF state was created, from which BS ($M_S = 0$) states were obtained. During geometry optimization, the internal geometries (but not their relative positions) of the methyl groups (all Cβ and Hβ atoms) of the acetates were fixed. All degrees of freedom were made available to all water molecules and the remaining atoms in the first ligand shell. The positions of all second- and third-shell amino acid side chains relative to the diiron site were fixed to those observed originally in the oxidized *M. capsulatus* protein structure.

Results and Discussion

Table 1 shows our DFT calculated properties for our largest model of Q as a function of both the spin state of the Fe sites and a ferromagnetic (F) or antiferromagnetic (AF) alignment of Fe spins. Fe spin states are described in terms of formal spins generated from the number of unpaired electrons on Fe. HS Fe sites that are F-coupled to give a maximum cluster spin of $S_{max} = 4$ are denoted by 2−2 (F) in Table 1. IS Fe sites that couple up to a cluster spin of $S = 2$ are referred to as 1−1 (F). Two possible BS states ($M_S = 0$) arise from the reorientation of the majority spin vector at a single Fe site; the 2−2 (AF) state is generated from a 2−2 (F) starting potential and the 1−1 (AF) state is created from the 1−1 (F) state.

Active Site Geometry Fe−Fe Distance. From Table 1, the HS 2−2 (F) state displays the longest Fe−Fe distance (2.73 Å). Spin flipping to the 2−2 (AF) state results in a shortening of the Fe−Fe distance (2.63 Å), consistent with early observations in which AF rather than F coupling was supposed important for the short Fe−Fe interaction. The freedom to obtain the spin coupling of the Fe sites from HS or IS sites leads to two additional states. In the 1−1 (F) state, the shorter Fe−Fe distance of 2.58 Å suggests that rather than direct AF coupling

(12) Lovell, T.; Li, J.; Noodleman, L. *Inorg. Chem.* **2001**, *40*, 5251−5266.
(13) Lovell, T.; Li, J.; Noodleman, L. *Inorg. Chem.* **2001**, *40*, 5267−5278.
(14) te Velde, G.; Bickelhaupt, F. M.; Baerends, E. J.; Fonseca, C. F.; van Gisbergen, S. J. A.; Snijder, J. G.; Ziegler, T. *J. Comput. Chem.* **2001**, *22*, 931−967.
(15) (a) Snijders, J. G.; Baerends, E. J.; Vernooijs, P. *At. Nucl. Data Tables* **1982**, *26*, 483. (b) Vernooijs, P.; Snijders, J. G.; Baerends, E. J. *Slater Type Basis Functions for the Whole Periodic System*; Internal report: Free University of Amsterdam: Amsterdam, The Netherlands, 1981.
(16) Krijn, J.; Baerends, E. J. *Fit Functions in the HFS-method*; Internal report (in Dutch): Free University of Amsterdam: Amsterdam, The Netherlands, 1984.
(17) (a) Boerrigter, P. M.; te Velde, G.; Baerends, E. J. *Int. J. Quantum Chem.* **1988**, *33*, 87−113. (b) te Velde, G.; Baerends, E. J. *J. Comput. Phys.* **1992**, *99*, 84−98.
(18) Versluis, L.; Ziegler, T *J. Chem. Phys.* **1988**, *88*, 322−328.
(19) Schlegel, H. B. In *Ab initio Methods in Quantum Chemistry*−I; Lawley, K. P., Ed; Advances in Chemical Physics; Wiley: New York, 1987; Vol. 67.
(20) Vosko, S. H.; Wilk, L.; Nusair, M. *Can. J. Phys.* **1980**, *58*, 1200−1211.
(21) Perdew, J. P.; Chekavry, J. A.; Vosko, S. H.; Jackson, K. A.; Perderson, M. R.; Singh, D. J.; Fioihais, C. *Phys. Rev. B* **1992**, *46*, 6671−6687.
(22) Noodleman, L. *J. Chem. Phys.* **1981**, *74*, 5737−5743.

Table 1. Geometries (Å), Fe Coordination Numbers, Net-Spin Populations, Heisenberg J Values (cm^{-1}), Directly Calculated Relative Energies (ΔE) (kcal/mol), Spin-Projected Relative Energies (ΔE_0) (kcal/mol), Average Isomer Shifts (δ) (mm/s), and Average Quadrupole Splittings (ΔE_Q) (mm/s) for High-Spin (2−2) and Intermediate-Spin (1−1) Fe Sites in Q

	formal spins associated with Fe1–Fe2			
geometry	1–1 (AF)	1–1 (F)	2–2 (AF)	2–2 (F)
Fe1−Fe2	2.42	2.58	2.63	2.73
Fe1−O1	1.72	1.78	1.77	1.75
Fe2−O1	1.86	1.76	1.77	1.85
Fe1−O2	1.91	1.80	1.83	2.09
Fe2−O2	1.71	1.77	1.75	1.72
Fe1−Oϵ1(Glu144)	2.07	2.11	2.35	2.20
Fe2−Oϵ2(Glu144)	1.95	1.96	2.02	2.12
Fe1−Nδ1(His246)	2.03	2.14	2.17	2.22
Fe2−Nδ1(His147)	2.15	2.10	2.13	2.12
Fe1−Oϵ2(Glu209)	1.90	1.86	1.87	1.85
Fe2−Oϵ1(Glu114)	1.92	1.91	1.90	1.88
Fe1−Oϵ1(Glu243)	1.96	1.97	2.06	1.97
Fe2−Oϵ2(Glu243)	2.00	2.04	2.20	2.40
Fe coordination no.	6	6	5	5
net spin population Fe1	1.27	1.54	−2.72	3.07
net spin population Fe2	−1.27	1.50	2.54	2.99
ΔE	7.53	3.99	0.00	11.82
J	−118		−376	
ΔE_0	10.83	8.00	0.00	15.82
Mössbauer δ	0.06	0.16	0.21	0.23
Mössbauer ΔE_Q	1.26	0.70	0.87	0.48

being the major cause, the abrupt shortening of the Fe−Fe distance is influenced subtantially by the presence of two IS Fe sites.[23] If AF coupling is the additional criterion governing the Fe−Fe distance, the corresponding 1−1 (AF) state should display an even shorter Fe−Fe distance.[11] In combination, IS Fe sites and AF coupling do shorten the Fe−Fe distance further to an EXAFS-compatible 2.42 Å for the 1−1 (AF) state, but at a significant energy cost (as discussed later). Of the four states examined, the asymmetry in Fe−O bond lengths observed from EXAFS is most clearly reproduced in the 1−1 (AF) state.

Coordination Number. The imidazole rings of both histidines are assumed to remain coordinated to Fe. The principal changes in the ligand array are therefore likely to occur in the more mobile, oxygen-based Glu side chains. Fe^{IV}−L (L = oxygen-based coordinating ligand) bond lengths of 2.2 Å or greater are potentially the weakest interactions and give rise to "open" coordination sites. From the bond lengths in Table 1, each Fe site is six coordinate for the 1−1 (F) and 1−1 (AF) states. A lengthening in the axially coordinated Fe1−$O_{\epsilon 1}$(Glu144) (2.20 Å) and Fe2−$O_{\epsilon 2}$(Glu243) (2.40 Å) bonds results in two five-coordinate Fe sites in the 2−2 (F) state. On the basis of the Fe1−$O_{\epsilon 1}$(Glu144) (2.35 Å) and Fe2−$O_{\epsilon 2}$(Glu243) (2.20 Å) bond lengths, Jahn−Teller-type distortions in the 2−2 (AF) state also produce two five-coordinate Fe sites. In the oxidized *M. capsulatus* protein environment and in our quantum cluster model, both $O_{\epsilon 1}$(Glu144) and $O_{\epsilon 2}$(Glu243) are hydrogen bonded: $O_{\epsilon 1}$(Glu144) to the side chain of Gln140 and $O_{\epsilon 2}$(Glu243) to the second-shell Wat785. These hydrogen bonding partners compete for residual OCO^- electron density with Fe, resulting in longer Fe1−$O_{\epsilon 1}$(Glu144) and Fe2−$O_{\epsilon 2}$(Glu243) bonds than would be anticipated for Fe^{IV}−$(CO_2)^-$ type interactions. Our calculations on the original model clusters omit these hydrogen bonding partners and the equivalent bond lengths are shorter. In the absence of structural changes in the protein environment during enzyme turnover, these hydrogen bonds would persist and lend support to the spectroscopic observations that Q displays two five-coordinate Fe species, but only when the Fe sites retain a HS configuration.

Net Spin Density at the Fe Sites. Net spin populations at the Fe sites serve as the primary indicator of HS or IS character associated with Fe. The calculated net spins in Table 1 are less than the pure theoretical values, indicative of substantial Fe-ligand covalency. For the 1−1 (F) state, spins on the irons amount to 1.54 and 1.50, consistent with the presence of two IS Fe sites. The 2−2 (F) state displays larger spin densities of 3.07 and 2.99, suggesting two HS Fe sites are present. The spins of these F-coupled states indicate the appropriate "spin parentage" of both the 2−2 (AF) and 1−1 (AF) states. For the 2−2 (AF) state, opposite signs in the calculated spin densities of −2.72 and 2.54 confirm AF coupling; the magnitude indicates two HS Fe sites. Spins of 1.27 and −1.27 on the irons of the 1−1 (AF) state are indicative of two AF-coupled IS Fe sites; the reduced spin density on the irons suggests this state is quite distinct from the 2−2 (AF) alternative.

Gas-Phase Energies. With regard to the sensitivity of our Q model to the Fe spin state, the 2−2 (AF) BS (0.0 kcal/mol) state is lower in energy than the 1−1 (F) (+4 kcal/mol), 1−1 (AF) (+8 kcal/mol), or 2−2 (F) (+12 kcal/mol) states. Rather than the AF or F coupling of two IS Fe sites, the AF coupling of two HS Fe sites is preferred. This result is consistent with spectroscopy and the PW91 functional[21] therefore describes the relative energetics in a reliable fashion. This energetic ordering also serves to highlight that the most important residues from the protein environment are incorporated into our quantum cluster. The majority of the charged and polar interactions with the diiron site that would otherwise come from an electrostatics-based description of the protein environment or from a quantum mechanical/molecular mechanics-based (QM/MM) approach are encompassed within the calculations. On the basis of the available protein X-ray structures, the relative energies between states are therefore likely to remain unchanged by further embedding our cluster in a long-range description of the protein.

Energies after Spin Projection. The 2−2 (AF) and 1−1 (AF) BS states are not pure singlet states; contamination with $M_S = 0$ components of higher lying nonsinglet states occurs. The pure singlet-state energy can be extracted using spin projection techniques,[22] using eq 1

$$E_0 = [(S_{max} + 1)E_{BS} - E(S_{max})]/S_{max} \quad (1)$$

where S_{max} = the maximum spin state accessible by the system. The net spin populations in Table 1 indicate that for valid spin projection, one must define the most appropriate maximum spin state of the system. For the 2−2 (AF) state, $S_{max} = 4$; for the 1−1 (AF) state, $S_{max} = 2$. Spin projection stabilizes the 2−2 (AF) state by −4 kcal/mol; the true ground state then lies −16 kcal/mol lower in energy than the 2−2 (F) state, and −11 and −8 kcal/mol lower in energy than 1−1 (AF) (after spin projection) and 1−1 (F) states.

Heisenberg Exchange Constant. The Heisenberg exchange coupling constant (J) for isovalent Fe sites is calculated from the energy difference of the BS and HS states using eq 2

$$E_{HS}(S_{max} = S_1 + S_2) - E_{BS}(M_S = S_1 - S_2) = -4JS_1S_2 \quad (2)$$

(23) Lovell, T.; Stranger, R.; McGrady, J. E. *Inorg. Chem.* **2001**, *40*, 39−43.

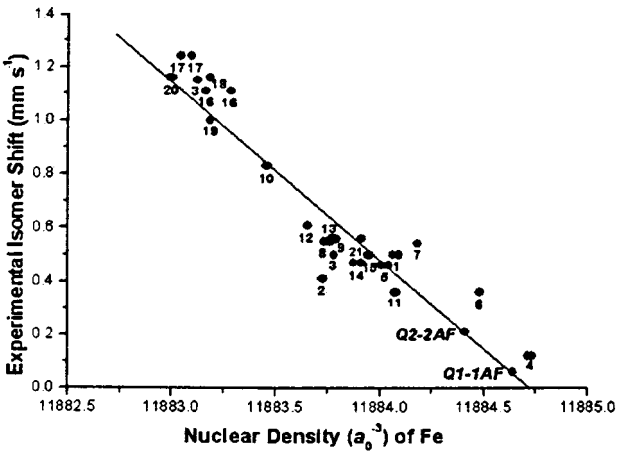

Figure 3. Linear correlation between measured isomer shifts and calculated electron densities for 15 dinuclear Fe-oxo, Fe-hydroxyl, and Fe-phenoxo-type compounds and 6 polar, mononuclear Fe complexes. Also shown are the predicted average 2−2 (AF) and 1−1 (AF) state values for our model of intermediate Q.

where $H = -2J\mathbf{S_1}\cdot\mathbf{S_2}$ and S_1 and S_2 are the site spin vectors on the adjacent Fe subunits, formally associated with the HS ferryl (S_1 and $S_2 = 2$) or IS ferryl (S_1 and $S_2 = 1$) ions. E_{HS} and E_{BS} are the gas-phase energies of the HS and BS states, respectively. For the 2−2 (AF) state, $J = -376$ cm^{-1}; for the 1−1 (AF) state, $J = -118$ cm^{-1}. These values are in reasonable accord, both in sign and magnitude, with the estimation from Mössbauer spectroscopy ($J < -30$ cm^{-1}) and that calculated by Dunietz et al. ($J = -143$ cm^{-1}) for a cluster similar to that in Figure 1a.[24]

Mössbauer Properties. To obtain Mössbauer parameters for our models of intermediate Q, we have recently rewritten our Hyper program, which calculates isomer shift and quadrupole splitting parameters and other properties in conjunction with the Amsterdam density functional code (ADF).[25,14] For the quadrupole splittings calculations, the standard ADF electric field gradient was used. To obtain reliable isomer shifts, all electron calculations were used to calculate the electron density at the Fe nuclei and a linear correlation was constructed between measured isomer shifts and calculated electron densities for a series of 15 dinuclear iron compounds plus 6 polar mononuclear iron complexes (Figure 3).[26]

For all the synthetic model complexes, experimental geometries were used and only the positions of the H atoms were optimized. The correlation between isomer shifts δ and Fe nuclear densities $\rho(0)$ is given in eq 3.

$$\delta = \alpha(\rho(0) - 11884.0) + C \qquad (3)$$

The best fit equation gives a correlation coefficient (r) of −0.94 with a standard deviation (SD) of 0.11 mm/s. Isomer shifts range from 1.2 to 0.14 mm/s for mainly high-spin Fe(II), Fe(III), and Fe(IV) sites. Also included in the series of 21 complexes is the intermediate-spin, F-coupled Fe_2O_2(5-Et$_3$-TPA)$_2^{3+}$ complex. The resulting fit ($\alpha = -0.664$, $C = 0.478$) was used to predict the isomer shifts for the Fe sites in the AF-coupled models of intermediate Q (Figure 2). This type of linear correlation approach has also been found to give a very good linear fit for isomer shifts in Fe−S complexes ($r = -0.95$, SD = 0.05 mm/s).[27] Experimental isomer shifts of 0.21 and 0.14 mm/s (*M. capsulatus*) and 0.17 and 0.17 mm/s (*M. trichosporium*) for sites Fe1 and Fe2, respectively, average in both cases to approximately 0.18 mm/s. For the 2−2 (AF) system, isomer shifts of 0.35 and 0.07 mm/s are calculated for sites Fe1 and Fe2; the corresponding 1−1 (AF) system gives much lower isomer shifts of 0.10 and 0.02 mm/s. In Table 1, the average isomer shift for the 2−2 (AF) state (0.21 mm/s) is clearly in much better agreement with experiment than the 1−1 (AF) alternative (0.06 mm/s), consistent with our energetics results.

We have also calculated quadrupole splittings (QS) for the mononuclear and dinuclear iron complexes cited in ref 26. The calculated QS are usually in good agreement with experiment. Typical RMS deviations are 0.3 mm/s (10−20%). With a linear fit, the standard deviation = 0.1 mm/s for QS. This level of accuracy is necessary for distinguishing between DFT calculated structural and electronic models for intermediate Q in MMOH. Reported experimental QS values are 0.68 and 0.55 mm/s (average = 0.62 mm/s) for *M. capsulatus and* 0.53 mm/s for both Fe sites in *M. trichosporium*. In the 2−2 (AF) system, calculated QS are 1.10 and 0.63 mm/s for Fe1 and Fe2, respectively; in the 1−1 (AF) state, the calculated QS of 0.92 and 1.60 mm/s are larger. Consistent with our isomer shift predictions, in Table 1 the average quadrupole splitting for the 2−2 (AF) state (0.87 mm/s) displays a better agreement with experiment than its 1−1 (AF) counterpart (1.26 mm/s). To our knowledge, these calculations represent the first DFT estimates of the isomer shift and quadrupole splitting parameters for models of intermediate Q of MMOH. The approach employed has general applicability and should be equally valuable in estimating Mössbauer parameters for intermediate X of the related binuclear non-heme enzyme, ribonucleotide reductase.

Summary

Our best model of Q displays two strongly AF-coupled five-coordinate HS Fe sites separated by 2.63 Å. While consistent with Mössbauer and XAS spectroscopy, the calculated Fe−Fe distance is longer than the EXAFS-derived range (2.46−2.52 Å).[7,8] The extensive charged hydrogen-bonding framework creates a more open structure than those considered previously (Figure 1) and should facilitate charge transfer (CT) into and out of the diiron cluster. In that respect, hydrogen bond shifts and CT to the second-shell ligands may be relevant to subsequent steps in the catalytic cycle. On the basis of our calculations, the presence of HS metal ions and a very short Fe−Fe separation as well as substantial asymmetry in the Fe−O bond lengths (from EXAFS) are mutually incompatible. EXAFS is often quite accurate for Fe−ligand and Fe−Fe distances; however, errors of up to 0.2 Å compared to subsequent X-ray structures have been found for Fe−Fe distances in some synthetic systems.[8] In this context, our calculated distance of

(24) Dunietz, B. D.; Beachy, M. D.; Cao, Y.; Whittington, D. A.; Lippard, S. J.; Friesner, R. A. *J. Am. Chem. Soc.* **2000**, *122*, 2880−2889.
(25) Liu, T.; Case, D. A.; Noodleman, L. *Hyper 2000*: Mössbauer isomer shifts, quadrupole splittings and hyperfine properties on metal and ligand centers for use with ADF; April 2001; Scripps internal report and code.
(26) Complexes: 1. $Fe_2(OH)(OAc)_2(HBpz_3)_2^{1+}$; 2. $Fe_2O(OAc)_2(bipy)_2Cl_2$; 3. $Fe_2(BPMP)(OPr)_2^{2+}$; 4. Fe_2O_2(5-Et$_3$-TPA)$_2^{3+}$; 5. $Fe_2O(Me_3TACN)_2(Cl_4cat)_2$; 6. $FeCl_4^{1-}$; 7. $Fe(bipy)_2Cl_2^{1+}$; 8. $Fe_2(salmp)_2$; 9. $Fe_2(Cat)_4(H_2O)_2^{2-}$; 10. $Fe_2(salmp)_2^{1-}$; 11. $Cl_3FeOFeCl_3^{2-}$; 12. FeF_6^{3-}; 13. $Fe_2O(OAc)_2(HBpz_3)_2$; 14. $Fe_3O(OAc)_2(Me_3TACN)_2^{2+}$; 15. $Fe_2O_2(6TLA)_2^{2+}$; 16. $Fe_2(salmp)_2^{2-}$; 17. $Fe_2(BPMP)(OPr)_2^{1+}$; 18. $Fe(Py)_4Cl_2$; 19. $FeCl_4^{2-}$; 20. $Fe_2(OH)(OAc)_2(Me_3TACN)_2^{1+}$; 21. $FeCl_6^{3-}$.
(27) Lovell, T.; Li, J.; Liu, T.; Case, D. A.; Noodleman, L. *J. Am. Chem. Soc.* **2001**, *123*, 12392−12410.

2.63 Å would appear reasonable. We also note that an excited state in which two IS, six-coordinate, AF-coupled, asymmetrically bridged Fe sites are separated by 2.42 Å lies +7.5 kcal/mol higher in energy and +11 kcal/mol higher after spin projection. More extensive studies in the protein are underway to examine the properties of these alternative electronic states in detail.

Acknowledgment. We thank NIH for financial support (GM43278 to L.N.), Per Siegbahn for stimulating discussions and suggesting this problem and E.J. Baerends and the Amsterdam group for use of the ADF codes.

Supporting Information Available: Structures of the quantum cluster models (PDF). This material is available free of charge via the Internet at http://pubs.acs.org.

JA0121282